Proceedings of the 28th IEEE
EMBS Annual International Conference
New York City, USA, Aug 30-Sept 3, 2006

Detection of lesions in retina photographs based on the wavelet transform

Gwénolé Quellec, Mathieu Lamard, Pierre Marie Josselin, Guy Cazuguel, Béatrice Cochener, Christian Roux

***Abstract*— In this article, we propose an automatic diabetic retinopathy screening method. In particular, we focus on detecting microaneurysms in retina photographs, as they are the most common and first appearing lesions in the disease development. This is done by matching a lesion template in the wavelet domain, using the sum of the squared errors as a criterion on some decomposition subbands. The method outperforms classification methods in the wavelet domain, which seem unfitted to describe small structures shapes. More, it could be generalized to other small lesions. Results are evaluated on a manually segmented retinal images database for different usual mother wavelets.**

***Index Terms*— diabetic retinopathy, microaneurysms, template matching, wavelet domain, usual mother wavelets**

I. INTRODUCTION

Images have always been used in medicine for teaching, diagnosis, and management purposes. Now medical imaging systems produce more and more digitized images in all medical fields: visible, ultrasound, X-ray tomography, MRI, nuclear imaging, etc... Thus for instance, Lund University hospital produces 15,000 new digital X-ray images per day [1]. These images are very interesting for diagnostic purposes: they are directly related to the patient pathology and medical history. However the amount of images we can access nowadays is so huge that database systems require efficient indexing to enable fast access to images in databases. In the same time, there is also a need for automatic screening for specific lesions in medical images to improve early detection of pathologies.

It is the case for diabetic retinopathy (DR). DR becomes a major public health issue because it is one of the main sources of blindness. Particularly, epidemiological studies carried out in industrialized countries classified DR amongst the four main causes of sight problems over the whole population and the first cause of blindness before 50 years old [2][3]. Economical issues are also at stake. As an example, 600 million dollars could be potentially saved every year in the United States by improving early detection of DR [4].

Gwénolé Quellec, Mathieu Lamard, Pierre Marie Josselin, Guy Cazuguel, Christian Roux and Béatrice Cochener are with Laboratoire de Traitement de l'Information Médicale Inserm U650, CHU Morvan Bat 2 Bis, 5 avenue Foch 29609 Brest Cedex France. gwenole.quellec@enst-bretagne.fr

Pierre Marie Josselin and Béatrice Cochener are with Service d'Ophtalmologie CHU Morvan, 5 avenue Foch 29609 Brest Cedex, France

Guy Cazuguel and Christian Roux are with Dpt Image et Traitement de l'Information, GET-ENST Bretagne, Technopole de Brest-Iroise CS 83818 - 29238 Brest Cedex, France

In the ophthalmology field, photographs often require time-consuming interpretations and classifications in order to adequately guide medical therapy. Automating this task would make it possible to detect diabetic retinopathy at a larger scale.

We introduce in this article an algorithm based on the wavelet transform and template matching. One of its advantages is that, once the wavelet transform is performed, it does not require further image preprocessing.

The proposed detection algorithm is evaluated on a database of green filtered retinal photographs.

II. MATERIAL AND METHOD

A. The database

Fig. 1. An example of (contrast enhanced) retinal photographic image

The database contains retinal images of diabetic patients, with associated anonymized information on the pathology. Diabetes is a metabolic disorder characterized by sustained inappropriate high blood sugar level. This progressively affects the conditions of many organs blood vessels, which may lead to serious renal, retinal, cardiovascular and cerebral complications. Like any other organ in the body, retina receives nutrition through blood vessels. In diabetes, these blood vessels are damaged engendring lesions that may lead to blindness. An example of retinal photographic image is given figure 1.

Diabetic retinopathy is an evolutive pathology, in which new kinds of lesions appear at each step. Microaneurysms

are the first lesions to appear. Amongst the different imaging modalities, photographs are the easiest and quickest, hence the interest of working on photographs alone, although diagnostic is quite difficult using only this modality, especially in earlier DR stage. Our database includes 995 images, with photographs and angiographs. Images have a definition of 1280 pixels/line for 1008 lines/image. They are lossless compressed images. The proposed screening algorithm needs a learning step, which is performed on images manually segmented by an expert.

B. The wavelet transform

Wavelets are families of functions generated from one single prototype function (mother wavelet) by dilation and translation operations: The mother wavelet is constructed from the so-called scaling function, satisfying the two-scale difference equation

$$\phi(t) = \sqrt{2} \sum_{k=-\infty}^{\infty} h(k)\phi(2t-k)$$

where $h(k)$ are the wavelet coefficients. Then, the mother wavelet $\psi(t)$ is defined as

$$\psi(t) = \sqrt{2} \sum_{k=-\infty}^{\infty} g(k)\phi(2t-k)$$

where $g(k) = (-1)^k h(1-k)$ [5]. Several different sets of coefficients $h(k)$ can be found, which are used to build a unique and orthonormal wavelet basis [5]. The wavelet transform represents the decomposition of a function into a family of wavelet functions $\psi_{m,n}(t)$ (where m is the scale/dilation index and n the time/space index). In other words, using the wavelet transform, any arbitrary function can be written as a superposition of wavelets.
Many constructions of wavelets has been introduced in the mathematical [6] and in the signal processing litterature (in the context of quadrature mirror filters) [7]. In the mid eighties, the introduction of multiresolution analysis and the fast wavelet transform by Mallat and Meyer provided the connection between the two approaches [8]. The wavelet transform may be seen as a filter bank and illustrated as follows, on a one dimensional signal x[n]:

- x[n] is high-pass and low-pass filtered, producing two signals d[n] (detail) and c[n] (coarse approximation)
- d[n] and c[n] may be subsampled (decimated by 2: $\downarrow 2$), otherwise the transform is called translation invariant wavelet transform
- the process is iterated on the low-pass signal c[n]

This process is illustrated on figure 2. We have then extracted information (subbands) at several scales plus an approximation of the signal (the last c[n]).

In the case of images, the filtering operations are both performed on raws and columns, leading to decomposition shown in figure 3.

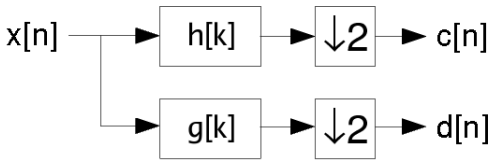

Fig. 2. Two-channel filterbank involving subsampling

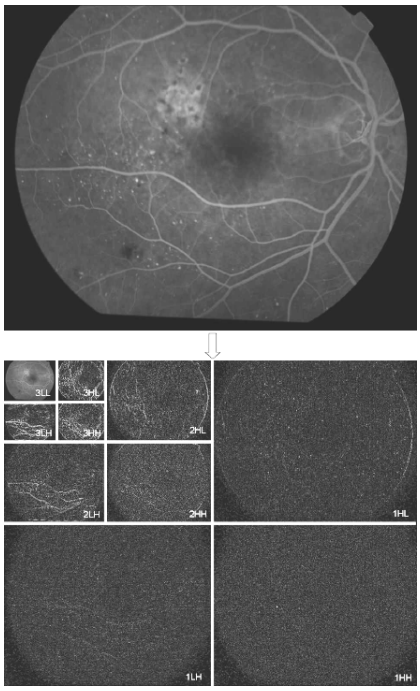

Fig. 3. Wavelet transform of an image
There are three subbands at each scale, depending on wether the raws/colums were high-passed or low-passed

C. Template matching in the wavelet domain

To evaluate the disease severity level, one must count the number of detected lesions. For this purpose, we move a window over an image and evaluate how close to a given type of lesion the local image area is. We first considered a generic classification of the wavelet transform coefficients of the image over all subbands, using several classifiers such as k-nearest neighbors or SVM. We evaluated several wavelet based shape/textural descriptors:

- the wavelet coefficients themselves, over all subbands
- the geometrical moments of the wavelet transforms
- fractional brownian motion estimators

Although this method seems to be adapted to large lesions with significant textural content, not any feature was discriminant enough to detect small lesions with varying size and intensity such as microaneurysms.
In fact, despite their size and intensity variations, microaneurysms are quite self-similar. Indeed, we can model them with a noisy 2-dimensional generalized gaussian function, with a constant shape parameter β and varying standard deviation α and amplitude. A generalized gaussian function

with unit amplitude is a function of the form (see figure 4):

$$f(x;\alpha,\beta) = \exp\left(\left(\frac{|x|}{\alpha}\right)^{\beta}\right)$$

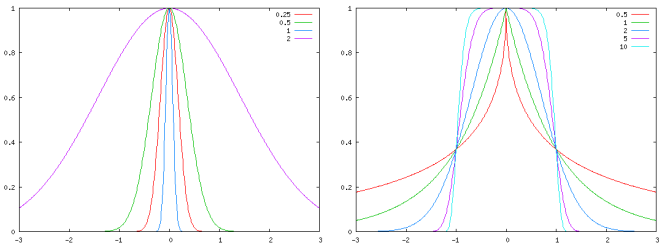

Fig. 4. Generalized gaussian function
The first plot (on the left) illustrates the role of the parameter α, the second the role of β

We can then move a window over an image to be classified and match a microaneurysm template. A similar approach has already been proposed to detect pulmonary nodules in Helical CT Images, using a gaussian function as template in the spatial domain [9]. Anyway, in our case, images present brightness variability, local background intensity variations and noise that would make it difficult to efficiently fit this model to a microaneurysm directly in the spatial domain. We get round this problem by fitting the wavelet transform of the model (WTM) on the wavelet transform of the image instead of fitting the original model on the raw image, and considering only interesting subbands. Indeed, by ignoring the high frequency subbands, we can get rid of the noise, and ignoring the low frequency subbands, we can get rid of slow image variations.
More precisely, for some given standard deviations (n different values), we compute the sum of the squared errors between the image and the WTM for some given amplitudes and record the smallest. As a result, we obtain n distance feature images. We then assume that a moving window is centered on a microaneurysm if, for at least one of the distance feature images, the corresponding distance is below a treshold. The tresholds are learned on a subset of the manually segmented lesions. In practice, the use of n=2 standard deviations are enough to represent the size variability of microaneurysms, provided that we don't use tough tresholds. The template parameters (fixed generalized gaussian shape parameter β, ranges for standard deviations α values and intensity relative amplitudes) are determined by analyzing images profiles on the learning subset of images. The models and an example of their decomposition are drawn on figure 5.

This method is somehow generical, as it is adapted to microaneurysm detection on both color photographs (with a negative model function amplitude) and angiographs (another image modality) and could be used to detect punctiform hemorrhages. Finally, as the studied lesions typical size is small (around 10 pixels of diameter on our images), the use of subsampled wavelet transform would lead to:

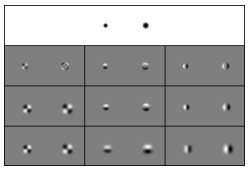

Fig. 5. The models and their decomposition
The models (first raw) are decomposed on three levels (one by raw). The decomposition directions are displayed column by column. Positive values are represented in white, negative values in black. The following parameters were used: $\beta = 4$, $\alpha = 2.5$ (small model) and $\alpha = 3.5$ (bigger model).

- too small transformed lesions on the interesting subbands, starting with the second level in wich subband dimensions are four times smaller than the raw image's.
- a translation variant template shape making it impossible to match the model.

Consequently, we used translation invariant wavelet transform (also known as undecimated wavelet transform) [10], in wich every subband have the size of the raw image.

D. Description of the overall procedure

1) *Building of the learning databases*: at the process beginning, examples of each lesions are manually detected by experts in images. As we are mainly interested in early detection of diabetic retinopathy, we focused on the first appearing lesions: microaneurysms.

2) *Optimization process*: the optimization process consists in adjusting a vector of tresholds. Its goal is to find the thresholds minimizing the number of detection errors on the set of learning images, segmented manually by the physician. For these images, we first compute the corresponding distance feature images. The optimal tresholds vector is then evaluated on the remaining images. As the process is not time consuming, we conducted a grid search optimization. It means that we explore the space of treshold tuples with a given step.
It is important to notice that, when optimizing the tresholds vector, we actually have two fitness criteria: sensitivity (percentage of detected lesions) and specificity (percentage of relevant detections) wich may be conflicting. Then, optimization consists in finding the best compromise between the two. In [11], the authors combine the two objective scores as follows:

$$\text{score} = \sqrt{sensitivity \times specificity}$$

Anyway, as in a disease screening framework the cost of false negatives is higher than that of false positives, we decided to favour sensitivity in our fitness criterion by aggregating the two fitness scores as follows:

$$\text{score} = \alpha \times \text{sensitivity}^2 + (1-\alpha) \times \text{specificity}^2,\ \alpha > \frac{1}{2}$$

3) *Performance evaluation*: once an optimal treshold vector is found, it is evaluated over the whole set of images. In that purpose, we compute the couple sensitivity/specificity for each annoted image in the database. As we are studying small structures, wavelets with a small support must be better fitted, for the local information is less diluted across space.

So, we have evaluated the method for well-knowned mother wavelets, with compact support:

- the haar wavelet
- the 5/3 biorthogonal wavelet (Le Gall wavelet), which is used in the Jpeg2000 standard part I [12]
- the Daubechies 4-tap orthogonal wavelet [13]

III. RESULTS

The evaluation scores are computed for each wavelet mentioned above and for each first four wavelet transform decomposition levels. In the particular case of level 0, the decomposed image is the original image itself: it will bring out the benefits of the wavelet transform in the pattern matching process. Concerning the other levels, we only consider the horizontal (high-passed raws/low-passed columns) and vertical (low-passed raws/high-passed columns) subbands, as the other subband (high-passed raws and columns) does not bring enough discriminant information. The results, computed on a subset of the database, are given in table I. An example of manual segmentation and automatic detection based on the second level of the Haar wavelet transform (the best combination) is given in figure 6.

level	Haar wavelet	5/3 biorthogonal wavelet	4-tap orthogonal wavelet
0	(52.60%,58.19%)	*idem*	*idem*
1	(81.23%,80.34%)	(36.53%,39.20%)	(59.49%,65.90%)
2	**(87.94%,96.18%)**	(75.48%,74.41%)	(72.88%,71.76%)
3	(65.42%,72.66%)	(75.56%,82.07%)	(22.76%,15.39%)

In each cell, the classification scores are given as a couple (sensitivity,specificity).
$sensitivity = \frac{number\ of\ detected\ lesions}{total\ number\ of\ lesions}$,
$specificity = \frac{number\ of\ detected\ lesions}{total\ number\ of\ detections}$

TABLE I
CLASSIFICATION SCORES

As expected, the best fitted wavelet, the Haar wavelet, has the most compact support. The results show that the method efficiency clearly depends on both the wavelet used and the decomposition level. They let us suppose that a better fitted wavelet may be found. We notice also that small hemorrhages are frequently detected as microaneurysms. This is not surprising: physicians themselves have difficulties to differentiate these lesions on photographs, without other information.

IV. CONCLUSION AND PERSPECTIVES

In this study, we have proposed a new method for detecting microaneurysms in retina. Given its simplicity and relative genericity, this method may be an answer for large screening of DR. But it must be possible to improve its efficiency by designing wavelets better fitted to special type of signals (corresponding to the studied lesions). We are working in this direction, coupled with a post-treatment task (template matching or classical pixel classification) especially designed for maximizing the separability between signal classes.

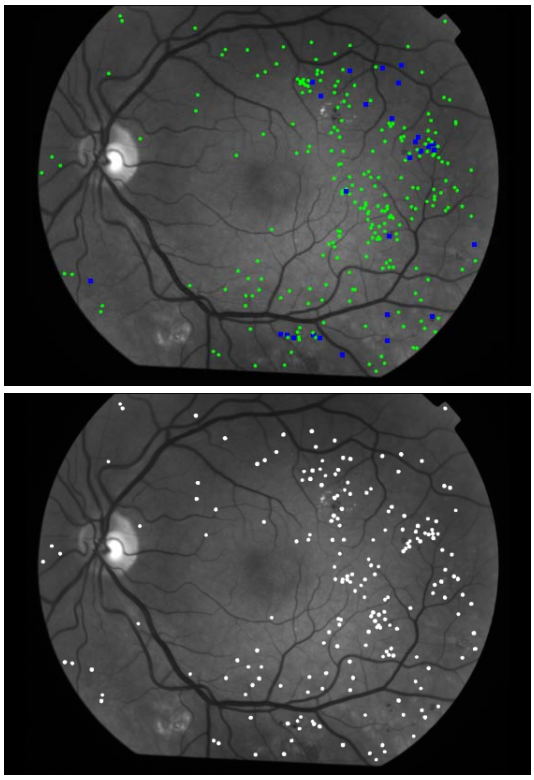

Fig. 6. Example of manually segmented image and detection result on a green filtered photograph.
On the manually segmented image (up image), microaneurysms are marked by dots and hemorrhages by bigger squares. The detected microaneurysms are shown on the bottom image.

REFERENCES

[1] *http://www.storagetek.com/solutions/case-studies/casestudy_page2136.html*.
[2] R. Klein, B. Klein, and S. Moss, "Visual impairment in diabetes," *Ophthalmology*, vol. 91, pp. 1–9, 1984.
[3] A. Sjolie, J. Stephenson, S. Aldington, E. Kohner, H. Janka, L. Stevens, J. Fuller, and the EURODIAB Complications Study Group, "Retinopathy and vision loss in insulin-dependent diabetes in europe," *Ophthalmology*, vol. 104, pp. 252–260, 1997.
[4] J. Javitt, "Cost savings associated with detection and treatment of diabetic eye disease," *Pharmacoeconomics*, vol. 8, pp. 33–9, 1995.
[5] S. Mallat, *A Wavelet Tour of Signal Processing*. Academic Press, 1999.
[6] J. Combes, A. Grossmann, and P. Tchamitchian, *Wavelets: Time-Frequency Methods and Phase Space*, 2nd ed. Springer-Verlag, 1989.
[7] T. Nguyen and P. Vaidyanathan, "Two-channel perfect-reconstruction fir qmf structures which yield linear-phase analysis and synthesis filters," *IEEE transactions on acoustics speech and signal processing*, vol. 37, no. 5, pp. 676–690, may 1989.
[8] S. Mallat, "Multifrequency channel decompositions of images and wavelet models," *IEEE transactions on acoustics speech and signal processing*, vol. 37, no. 12, pp. 2091–2110, 1989.
[9] Y. Lee, T. Hara, and H. Fujita, "Automated detection of pulmonary nodules in helical ct images based on an improved template-matching technique," *IEEE Transactions on Medical Imaging*, vol. 20, no. 7, pp. 595–604, 2001.
[10] R. R. Coifman and D. L. Donoho, "Translation-invariant de-noising," Department of Statistics, Tech. Rep., 1995.
[11] H. Shao, W. cheng Cui, and H. Zhao, "Medical image retrieval based on visual contents and text information," 2004.
[12] D. L. Gall and A. Tabatabai, "Subband coding of digital images using symmetric short kernel filters and arithmetic coding techniques," 1988.
[13] I. Daubechies, *Ten Lectures on Wavelets*. SIAM, 1992.